A THEORETICAL AND EXPERIMENTAL STUDY OF THE FLUID MOTION ABOUT A FLAT PLATE ROTATED IMPULSIVELY FROM REST TO A UNIFORM ANGULAR VELOCITY

FINAL REPORT

by

T. Sarpkaya
Department of Mechanical Engineering
University of Nebraska
Lincoln, Nebraska

Contract Nonr: 3718(03)
Project NR 6250887

December 1966
NU-Hydro-Report No: 027-1

The research was carried out under the Bureau of Ships General Hydromechanics Research Program, S-R009 01 01, administered by the David Taylor Model Basin.

ABSTRACT

This report presents the results of an experimental and theoretical investigation of separated unsteady flow about a flat plate (a fin or aileron) rotating impulsively from rest to a uniform angular velocity about an axis along its leading edge in an incompressible fluid otherwise at rest or moving steadily and uniformly about the plate. The results show that the early stages of motion are accompanied by torsional oscillations, the frequency of which is identical with the natural frequency of the submerged system. The initial hydrodynamic torque is determined by the added mass-moment of inertia of the plate. In the oscillatory stage of motion the torque is comprised of an angular-velocity-dependent form-torque and an acceleration-dependent inertial torque. These torque components are interdependent as well as time-dependent. The rotation of the plate in a steady uniform flow gives rise to a hinge moment which is considerably larger than that of a plate held fixed at the same instantaneous angle of incidence. The moment coefficient is determined by the instantaneous angle of attack and the rotation parameter $b\omega/U$. For a given angle of attack the hydrodynamic torque increases with increasing values of $b\omega/U$. The results are in conformity with the observations that when the angle of attack of an airfoil is rapidly increased (e.g., during maneuvering flight) the stall occurs at larger angles of attack.

NOMENCLATURE

a = half cord length, $b/2$

b = cord length, $b = 2a$

$C(\theta)$ = inertial torque coefficients

C_ω = form-torque coefficient

C_M = hinge moment coefficient, $T/\rho U^2/2\ b^2 h$

C_T = torque coefficient, $T/\rho b^4 h\omega^2$

$f(z)$ = complex function

h = span of flat plate

I = mass moment of inertia

R = radius

t = time

T = moment or torque

U = velocity of steady uniform flow

u, v = velocity components

$w(z)$ = a complex function

z = complex variable

Γ = circulation

ζ = complex variable

θ = angle of rotation

λ = dimensionless circulation, $\Gamma/2\pi a^2\omega$

ρ = density of fluid

ψ = stream function

ω = angular velocity

$\dot{\omega}$ = angular acceleration

$\dot{\omega}_o$ = amplitude of angular acceleration

PURPOSE AND SCOPE OF THE RESEARCH

The research described in this paper is a part of work initiated under the Bureau of Ships General Hydromechanics Research Program, administered by the David Taylor Model Basin, on separated unsteady flow about control surfaces rotating impulsively from rest to a uniform angular velocity about an axis along its leading edge.

The work involves (a) the study of the hydrodynamic torque, the growth and motion of vortices, and the torsional oscillations; (b) the extension of the results to control surfaces of finite span and to cases where a control surface is attached to the leading and trailing edge of a streamlined body; and finally, (c) the determination of the body-control surface interference and the turning characteristics of the leading body. The present report deals only with the first phase of the research, i.e., with the characteristics of two-dimensional plates rotating in a fluid at rest and in a uniform steady ambient flow.

INTRODUCTION

The separated flow about plates and various profiles at rest has been the subject of extensive investigation. The study of flow about rotating bodies, however, was concerned primarily with the development of laminar boundary layer on a disk, sphere, or a slender body of revolution rotating in a fluid at rest or in an axial stream.[1] In general it was found that the drag coefficient increases with increasing $R\omega/U$. The separated unsteady flow phenomena about flat plates rotating impulsively from rest to a uniform angular velocity in a fluid which is at rest or moving steadily and uniformly about the plate have not been investigated although such flows play a predominant role in the design and operation of control surfaces on flying, floating, or submerged bodies.

The theoretical studies of the non-uniform motion of airfoils and ailerons have been concerned primarily with the solution of the problems of wing flutter, gust loadings, flapping-wing flight, and accelerated flight in general. In developing the theory it has been assumed, among other things, that (a) the airfoil may be replaced by a flat plate; (b) the amplitude of oscillation is small; (c) the strength of circulation around the airfoil is such as to preclude flow around the trailing edge at all times; and that (d) the vortices in the wake remain fixed with respect to the undisturbed fluid. For a flat plate undergoing a finite rotation the assumptions of the flutter analysis are not valid. Consequently, the theoretical and experimental investigations of the moment and lift acting on airfoils, ailerons, or rudders at rest or undergoing

small amplitude oscillations, are of little help in the determination of torque and stability characteristics of control surfaces subjected to finite rotations.

The characteristics of the separated time-dependent flow are largely determined by the instantaneous angle of rotation θ, the rotation parameter $b\omega/U$, the amplitude of the angular acceleration $\dot{\omega}_o/\omega^2$, and the natural frequency of the submerged system. The results show that there are significant differences between the torque and wake characteristics of a plate rotating in a fluid at rest and those of a plate rotating in a steady uniform flow. When a flat plate is suddenly rotated about an axis along one of its edges to an angular velocity ω in an incompressible fluid otherwise at rest, it is observed that the boundary layer separates at the leading and trailing edges and two regions of vorticity break away from the edges and move away relative to the plate, beginning the formation of a wake. During the early stages of motion a torsional oscillation is superposed on the uniform rotation of the plate. The period of oscillation of the submerged system is determined by the added moment of inertia and the mass moment inertia of the plate in addition to its physical and geometrical characteristics.

When the plate, initially at zero angle of incidence, is suddenly rotated about its leading edge to an angular velocity ω in a uniform flow, the development of vortices is governed by the instantaneous angle of incidence and the rate of rotation. The rotational motion delays the separation of flow at the trailing edge, and this in turn gives rise to a hinge moment which is considerably larger than that

of a plate held fixed at the same instantaneous angle of incidence. Following the shedding of the first vortex the torque decreases rapidly at first and then oscillates with the frequency of vortex shedding as the rotation continues.

In terms of the two-dimensional unsteady problem, the regions of vorticity that separate from the boundary layer and move downstream are quite thin, justifying a description of them as vortex sheets. Furthermore these sheets roll up, concentrating most of the vorticity toward the downstream end of the sheet. The vortex sheet may be approximated by a single concentrated line vortex at the center of gravity of the vorticity while maintaining, conceptually, a connecting sheet of vanishingly small vorticity to the body. This description makes possible the formulation of a relation for the motion of vortices and the determination of the hydrodynamic torque acting on the plate.

THEORETICAL ANALYSIS

The Complex Potential for a Rotating Plate

The fluid motion about the plate in the z-plane (see Fig. 1) may be transformed into the exterior of a circle of radius "a" in the ζ-plane through the use of the transformation

$$f(\zeta) = z = \frac{1}{2}\left(\zeta + \frac{a^2}{\zeta}\right) \tag{1}$$

Then the complex function $F(z, \bar{z})$ for the plate (rotating clockwise) alone, i.e., excluding the vortices, may be written as

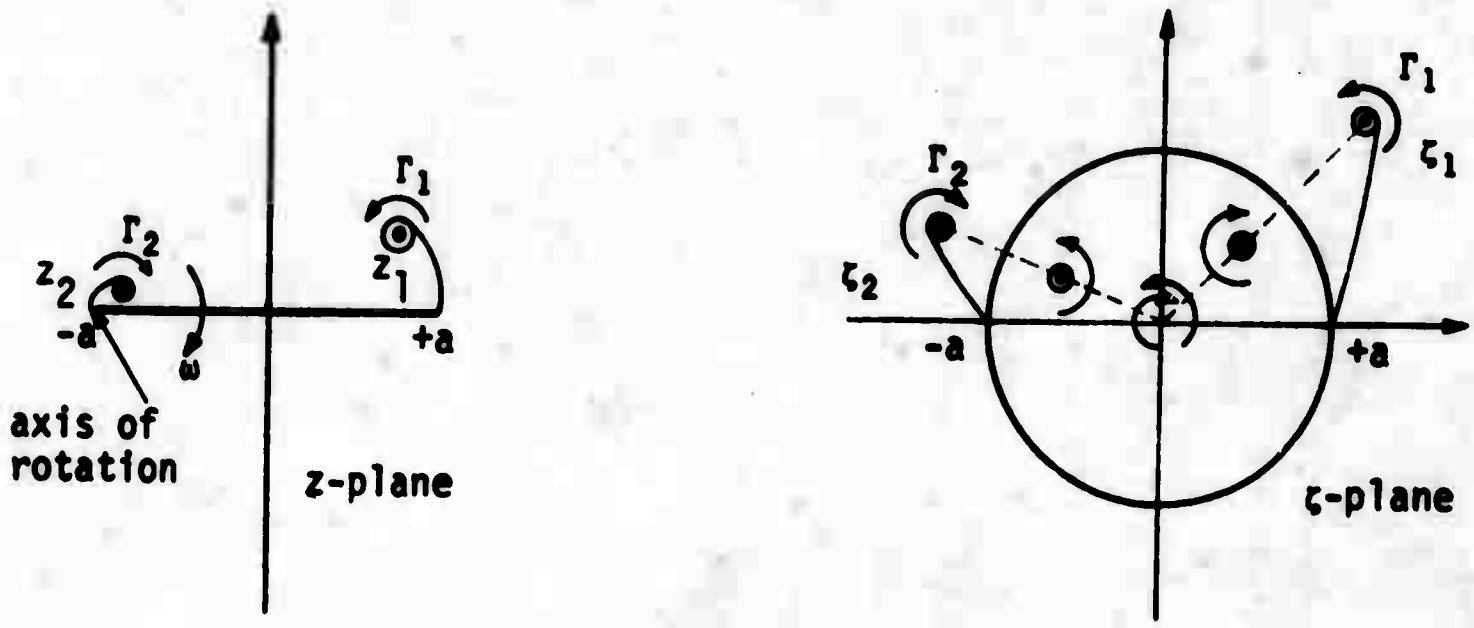

Fig. 1 Transformation Planes

$$F(z, \bar{z}) = -\frac{1}{2} i\omega z\bar{z} + i\omega \bar{z}_0 z \tag{2}$$

or

$$2i\psi = -i\omega z\bar{z} + 2i\omega z\bar{z}_0 \quad , \quad \bar{z}_0 = -a \tag{3}$$

Inserting the value of z in Eq. (3) from Eq. (1) and remembering that $\zeta\bar{\zeta} = a^2$ on the cylinder, one has the "Boundary Function" $B(\zeta)$[2]

$$B(\zeta) = 2i\psi = -\frac{i\omega}{4}(\zeta + \frac{a^2}{\zeta})(\frac{a^2}{\zeta} + \zeta) - ia\omega(\zeta + \frac{a^2}{\zeta}) \tag{4}$$

Simplifying, one has

$$B(\zeta) = B_1(\zeta) + B_2(\zeta) = -\frac{i\omega}{4}(\zeta^2 + 4a\zeta + 2a^2)$$

$$-\frac{i\omega a^2}{4}\left(\frac{a^2}{\zeta^2} + 4\frac{a}{\zeta}\right) \tag{5}$$

where

$$B_2(\zeta) = w = -\frac{i\omega a^2}{4}\left(\frac{a^2}{\zeta^2} + 4\frac{a}{\zeta}\right) \tag{6}$$

The function $B_2(\zeta)$ or w in Eq. (6) contains all the negative powers of ζ and no non-negative powers. Thus w is holomorphic outside the circle, vanishes at infinity, and satisfies the boundary conditions. Consequently, w is the complex function which represents the potential flow, without the vortices, about the flat plate rotating in the clockwise direction about its one edge.

Added Moment of Inertia and Torque for Unseparated Flow

The kinetic energy of fluid (for plate length h) is given by

$$E = -\frac{1}{4}i\rho h \int_C w d\bar{w} \tag{7}$$

taken around the plate or the cylinder boundary c, hence

$$E = -\frac{1}{4} i\rho h \int_c \frac{a^4\omega^2}{8}\left(\frac{a^2}{\zeta^2} + \frac{4a}{\zeta}\right)\left(\frac{\zeta}{a^2} + \frac{2}{a}\right) d\zeta \qquad (8)$$

Performing the indicated integration, one has

$$E = \frac{9}{16}\pi\rho a^4 h\omega^2 \qquad (9)$$

Since

$$\frac{dE}{dt} = I\omega\frac{d\omega}{dt} = \frac{9}{8}\pi\rho a^4 h\omega\frac{d\omega}{dt} \qquad (10)$$

the "added moment of inertia" I reduces to

$$I = \frac{9}{8}\pi\rho a^4 h \quad , \quad \text{or} \quad I = \frac{9}{8}\pi\rho\left(\frac{b}{2}\right)^4 h \qquad (11)$$

Consequently, the initial torque acting on the plate prior to the formation of vortices is given by

$$T = \frac{9}{8}\pi\rho a^4 h\frac{d\omega}{dt} \qquad (12)$$

In terms of the torque coefficient expressed by

$$C_T = \frac{\text{Torque}}{\rho b^4 h\omega^2} \qquad (13)$$

Equation (12) reduces to

$$C_T = \frac{9\pi}{128} \frac{\alpha}{\omega^2} \quad \text{with} \quad \alpha = \frac{d\omega}{dt} \tag{14}$$

Equation (14) will be referred to later in connection with the evaluation and discussion of experimental results.

Analysis of Vortex Motion

The total complex potential function describing the rotation of the plate and the two vortices located above the plate may be written as,

$$F = -\frac{ia^2\omega}{4}\left(\frac{a^2}{\zeta^2} + 4\frac{a}{\zeta}\right) + \frac{i\Gamma_1}{2\pi} \operatorname{Ln}(\zeta - \zeta_1) - \frac{i\Gamma_1}{2\pi} \operatorname{Ln}(\zeta - \frac{a^2}{\bar{\zeta}_1})$$

$$- \frac{i\Gamma_2}{2\pi} \operatorname{Ln}(\zeta - \zeta_2) + \frac{i\Gamma_2}{2\pi} \operatorname{Ln}(\zeta - \frac{a^2}{\bar{\zeta}_2}) + \frac{i}{2\pi}(\Gamma_1 - \Gamma_2) \operatorname{Ln}\zeta \tag{15}$$

F is made up of the potentials due to (a) rotation of plate, (b) the two vortices in the wake, and (c) the "reflection of the two vortices" in the cylinder. The last term in Eq. (15), while correctly obtained by the circle theorem, is henceforth excluded by virtue of the condition that total circulation in the fluid region remains zero, i.e., a circulation of strength $(\Gamma_2 - \Gamma_1)/2\pi$ is set up around the plate.

In order that the flow described by the complex potential function F be compatible with the motion of the observed flows, the Kutta condition at the sharp edges where the sheet is fed must be satisfied. It simply states that the feeding points are stagnation points, i.e., the fluid velocity relative to the cylinder vanishes at these points.

Writing

$$\frac{dF}{d\zeta} = -\frac{ia^2\omega}{4}\left(-2\frac{a^2}{\zeta^3} - 4\frac{a}{\zeta^2}\right) + \frac{i\Gamma_1}{2\pi}\frac{1}{\zeta - \zeta_1}$$

$$-\frac{i\Gamma_1}{2\pi}\frac{1}{\zeta - \frac{a^2}{\bar{\zeta}_1}} - \frac{i\Gamma_2}{2\pi}\frac{1}{\zeta - \zeta_2} + \frac{i\Gamma_2}{2\pi}\frac{1}{\zeta - \frac{a^2}{\bar{\zeta}_2}} \qquad (16)$$

and $\frac{dF}{d\zeta} = 0$ at $\zeta = a$, we have

$$\frac{3}{2} + \lambda_1\frac{1}{1 - \frac{\zeta_1}{a}} - \lambda_1\frac{1}{1 - \frac{a}{\bar{\zeta}_1}} - \lambda_2\frac{1}{1 - \frac{\zeta_2}{a}} + \lambda_2\frac{1}{1 - \frac{a}{\bar{\zeta}_2}} = 0 \qquad (17)$$

where λ_1 and λ_2 are dimensionless strength of vortices and are defined by

$$\lambda_1 = \frac{\Gamma_1}{2\pi a^2 \omega} \quad , \quad \lambda_2 = \frac{\Gamma_2}{2\pi a^2 \omega} \tag{18}$$

Similarly, writing $\frac{dF}{d\zeta} = 0$ at $\zeta = -a$ in Eq. (16), we have

$$\frac{1}{2} - \frac{\lambda_1}{1 + \frac{\zeta_1}{a}} + \frac{\lambda_1}{1 + \frac{a}{\bar{\zeta}_1}} + \frac{\lambda_2}{1 + \frac{\zeta_2}{a}} - \frac{\lambda_2}{1 + \frac{a}{\bar{\zeta}_2}} = 0 \tag{19}$$

The Equations (17) and (19) express the Kutta condition at the trailing and leading edges of the plate respectively.

Force Balance Equations

In Fig. 1 the vortex sheet on the right was approximated by the concentrated vortex of circulation Γ_1 at z_1 and a feeding sheet of vanishingly small circulation connecting z_1 to the feeding point $z = a$ on the plate. Mathematically, there is a branch line between z_1 and $z = a$ and the velocity potential ϕ is discontinuous across this branch line, the discontinuity in ϕ being Γ_1, the circulation of the vortex. There is therefore a discontinuity in pressure across this branch line (alias vortex sheet) of amount $\rho\dot{\Gamma}_1$, the total (complex vector) force acting on this vortex sheet is therefore $i\rho\dot{\Gamma}_1(z_1 - a)$. The force acting on the concentrated vortex is $-i\rho\Gamma_1(W_1 - \dot{z}_1)$ where W_1 is the local fluid velocity vector at the vortex and $\dot{z}_1$ is the

velocity vector of the vortex. Thus to make the net force on the concentrated vortex and its feeding sheet vanish we must have[3]

$$i\rho\dot{\Gamma}_1(z_1 - a) - i\rho\Gamma_1(W_1 - \dot{z}_1) = 0 \tag{20}$$

or, in dimensionless form, one has

$$\frac{\dot{z}_1}{a\omega} + \frac{\dot{\lambda}_1}{\omega}\frac{1}{\lambda_1}\left(\frac{z_1}{a} - 1\right) = \frac{u_{z1} + iv_{z1}}{a\omega} \tag{21}$$

A similar analysis for the vortex and its feeding sheet on the left in Fig. 1, yields

$$\frac{\dot{z}_2}{a\omega} + \frac{\dot{\lambda}_2}{\omega}\frac{1}{\lambda_2}\left(\frac{z_2}{a} + 1\right) = \frac{u_{z2} + iv_{z2}}{a\omega} \tag{22}$$

Complex Velocities in the Physical Plane (z-plane)

The complex velocities appearing in Eqs. (21) and (22) may be determined from the complex function F by writing,

$$u_{z1} + iv_{z1} = -\frac{d\overline{F_1(z)}}{d\bar{\zeta}}\frac{d\bar{\zeta}}{d\bar{z}} + i\omega(a + z_1) \tag{23}$$

where

$$F_1(z) = F(z) - \frac{i\Gamma_1}{2\pi} \mathrm{Ln}(\zeta \quad \zeta_1) - \frac{i\Gamma_1}{2\pi} \mathrm{Ln}(1 - \frac{1}{\zeta\zeta_1}) \tag{24}$$

Similarly, the complex velocity for the vortex at $z = z_2$ is given by

$$u_{z2} + iv_{z2} = - \frac{d\overline{F_2(z)}}{d\bar{\zeta}} \frac{d\bar{\zeta}}{d\bar{z}} + i\omega(a + z_2) \tag{25}$$

where

$$F_2(z) = F(z) + \frac{i\Gamma_2}{2\pi} \mathrm{Ln}(\zeta - \zeta_2) + \frac{i\Gamma_2}{2\pi} \mathrm{Ln}(1 - \frac{1}{\zeta\zeta_2}) \tag{26}$$

Evaluation of Differential Equations

The Equations (17, 19, 21, 22, 23) and (25) represent a set of rather involved nonlinear first-order differential equations for the complex co-ordinates, strengths, and complex velocities of the two vortices. They were integrated, by finite difference approximation, on an IBM-7040 computer* with ωt increments of 0.005. Figure 2 shows the results of this calculation as the solid curve. The dotted line

---

*The IBM-7040 computer can perform mathematical operations with complex variables when the problem is programmed in Fortran-4 language.

shows the experimental results obtained from motion pictures. These results will be taken up later in connection with the "Discussion of Results and Conclusions".

EXPERIMENTAL EQUIPMENT

Experiments were conducted in a plexiglass reservoir (Fig. 3) and in a vertical water tunnel.

The reservoir was 4 ft high and had a 3 ft by 3 ft cross section. A 3 ft by 3 ft and 1 in. thick plexiglass plate was placed 2.005 ft above the bottom of the reservoir. The test plates (2 ft long, 0.25 in. thick, and b = 4, 5, 6, 7, and 8 in. wide plexiglass plates) were placed within this 2.005 ft high test section with very small clearances (0.03 in.) at top and bottom. The bottom end of the axis of rotation was placed in a self-aligning bearing buried in the bottom plexiglass plate and the top end was extended, with the help of another bearing, above the top plexiglass plate and rigidly connected to the torque meter.

The angular acceleration of the plate was measured with the aid of a cantilever-beam-mass system. The electrical outputs of both the acceleration meter and the torque transducer were fed into separate channels of an amplifier-recorder system.

The torque transducer-plate combination was rotated with a set of worm gears located directly above the acceleration meter. The driving system consisted of a variable speed motor, magnetic clutch-brake mechanism, and two timers. The clutch-brake mechanism was so wired that

when the clutch was engaged the brake automatically disengaged and vice versa.

The locations of vortices, both with respect to the plate and with respect to a fixed frame, were determined from motion pictures taken during several test runs. Since the motion picture frames were synchronized with the torque and acceleration meters through the use of the recorder marker, it was possible to correlate the instantaneous torque and the corresponding angle of rotation with the characteristics of vortices.

The vertical water tunnel,[4] which had a 2 ft-square cross section, was used in the investigation of the characteristics of flow about plates rotating in a uniform steady ambient flow. The test plate was initially set at zero angle of incidence. Following the establishment of a uniform ambient flow, the plate was rotated impulsively from rest to a uniform angular velocity about a horizontal axis coincident with the leading edge of the plate through the use of the driving system described above. The cord length of the test plates used in the tunnel was 4, 5, and 6 inches. The 6 in. plate was rotated no more than 40 degrees in order to minimize the tunnel and wake-blockage effects as much as possible. To reduce the effect of finite plate thickness (0.25 in.), at least for the larger angles of attack, the leading edge was rounded and the trailing edge was made sharp on the upstream side.

DISCUSSION OF RESULTS AND CONCLUSIONS

Rotation in a Fluid at Rest

One of the most distinguishing features of impulsively started uniform rotation in a fluid otherwise at rest is the superposition of a non-linear torsional oscillation on the uniform rotational motion. The oscillation is non-linear because both the added moment of inertia and the torsional damping coefficient vary with time due to the growth and motion of vortices. Experiments show that the torque acting on the plate oscillates with a frequency equal to the natural frequency of the torsional vibration of the submerged system.

The torque coefficient C_T, defined by Eq. (14) is valid only for unseparated flow and in general is a function of the initial angular acceleration and average angular velocity of the plate, both of which may be varied independently. The rotational oscillation of an otherwise uniformly rotating flat plate is, like those of other bodies, very much related to the formation and shedding of vortices at the sharp edges. At the start of motion the resisting torque is primarily due to induced moment of inertia and the mass moment of inertia of the plate since the vortices are negligibly small. As the motion continues, a wake forms and grows. The formation of the wake gives rise not only to a form-torque, as would be the case if the motion were steady, but also to significant changes in inertial forces. In other words, the angular-velocity and angular-acceleration-dependent torques are interdependent

as well as time dependent. Finally, they both depend upon the preceding history of the fluid motion.

This interpretation suggests that the total hydrodynamic torque could be written as

$$T = C_\omega \rho b^4 h \omega^2 + C_1 \frac{\pi b^2}{4} \rho b^2 h \dot{\omega} + C_2 \frac{\pi b^2}{4} \rho b^2 h \frac{\dot{\omega}}{\omega} + \ldots$$

or

$$C_T = \frac{T}{\rho b^4 h \omega^2} = C_\omega(\theta) + C_1(\theta) \frac{\pi}{4} \frac{\dot{\omega}}{\omega^2} + C_2(\theta) \frac{\dot{\omega}}{\omega^3} + \ldots$$

in which C_ω is the form-torque coefficient and C_1, C_2, . . . are the inertia coefficients. These coefficients are functions of the instantaneous angle of rotation only and, hence, a unique relationship should exist between them. At present a purely theoretical determination of the form and inertial torque coefficients appears to be quite difficult. For a rotation with constant angular acceleration $C_1(\theta) = 9/32$ at the start of motion, i.e., for $\theta = 0$.

Figure 4 shows the hydrodynamic torque coefficient C_T as a function of f.t for $\dot{\omega}_0/\omega^2 = 40$, as determined experimentally using flat plates of three different cord lengths. Also shown on this figure is the torque coefficient calculated from Eq. (14) using the independently measured instantaneous angular acceleration. During the early stages of motion the torque is almost purely inertial. Subsequently, the form-torque increases and, as the motion approaches a steady-state, the torque

coefficient becomes independent of both f.t and $\dot{\omega}_o/\omega^2$, and approaches approximately unity. No attempt has been made to separate, for the oscillatory stages of motion, the velocity dependent torque from the acceleration dependent torque since the effect of wake development on the added moment of inertia and hence on the coefficient of $\dot{\omega}/\omega^2$ in Eq. (14) has not yet been analyzed.

The theoretically and experimentally determined location of vortices relative to the plate was shown in Fig. 2. It is sufficient to note that the theoretical prediction is quite satisfactor despite the neglect of torsional oscillations and supports the hypothesis that viscosity, aside from being responsible for the formation and subsistence of the vortex layers emanating from the body, does not play a distinguishable role in the mechanism of growth and motion of vortices. Also shown in Fig. 2 is the strength of vortices. It is observed that the strength of the trailing edge vortex is considerably larger than that of the leading edge vortex. A careful examination of the motion pictures shows that the vortex sheet emanating from the trailing edge is comprised of a series of S-shaped local undulations. These undulations are generated by the vibration of the trailing edge of the plate and eventually rolled up into a series of small vortices along the feeding layer.

Rotation of Plate in Uniform Flow

As pointed out earlier, there are significant differences between the torque and wake characteristics of a plate rotating in a fluid at

rest and those of a plate rotating in a steady uniform flow. When the plate, initially at zero angle of incidence, is suddenly rotated in a uniform flow about its leading edge to an angular velocity ω, the flow separates from the leading edge and rolls up into a vortex at the suction side of the plate. The vortex is enclosed in a separation bubble extending from the leading edge to a stagnation point lying somewhere between the leading and trailing edges. Evidently, the main flow remains attached to the plate beyond the stagnation point. Eventually, the leading edge vortex grows so large that the entire suction side of the plate becomes one big separation bubble. With increasing angle of attack the center of the leading edge vortex moves farther downstream as seen in Fig. 5. When a critical angle of attack is exceeded, the circulation developed about the plate is not sufficient to prevent separation at the trailing edge. Then the flow separates from the trailing edge and forms a second vortex at the suction side of the plate. Eventually, the first vortex sheds and the flow attaches the plate at the leading edge while the trailing edge vortex continues to grow. The formation, growth, and motion of the trailing edge vortex causes a considerable change in pressure distribution along the plate and especially on the suction side. This in turn produces a rapid decrease in the moment.

The moment coefficient C_M, defined by $C_M = 2T/\rho U^2 b^2 h$, is a function of the instantaneous angle of rotation and the rotation parameter $b\omega/U$. Although C_M may be expressed in a form similar to that given for C_T, the variation of various coefficients with the instantaneous angle of

attack cannot be resolved, at least at present, theoretically. At the start of motion the flow is essentially of potential nature, and the hydrodynamic torque therefore is basically due to inertial forces. Then the moment coefficient has a theoretical value of $C_M = \frac{9\pi}{64}\left(\frac{b\omega}{U}\right)^2 \frac{\dot{\omega}_0}{\omega^2}$. Experiments show that the plate accelerates to a uniform angular velocity within a few degrees of rotation and the torsional oscillations, which are several orders of magnitude smaller than those discussed previously, damp out rapidly during the acceleration period. Consequently, the moment coefficient (see Fig. 6), corresponding to the values of θ between zero and the end of the acceleration period, was calculated by subtracting the theoretically calculated inertial torque $\frac{9\pi}{64}\left(\frac{b\omega}{U}\right)^2 \frac{\dot{\omega}}{\omega^2}$ from the actual torque measured. The portion of the C_M curves, which passed through the data points to which the above inertia correction procedure was applied, is shown by broken lines in Fig. 6.

It is observed that the moment coefficient rises to a maximum and then drops off rapidly as soon as the flow separates at the trailing edge. During the later stages of motion, (the plate is still rotating with a uniform angular velocity), the alternate shedding of vortices cause regular oscillations in the moment coefficient. It is noted that the moment coefficient reaches higher maximums with increasing values of $b\omega/U$. For very low values of $b\omega/U$, the moment coefficient approaches the quasi-steady state values. It is clear that control surfaces rotating in a steady uniform flow are subjected to considerably larger hinge moments than those held fixed at the same instantaneous angle of

incidence. This finding is in conformity with the observations concerning the lift force, i.e., when the angle of attack of an airfoil is rapidly increased the stall occurs at larger angles of attack.

REFERENCES

1. H. Schlichting, Boundary Layer Theory, McGraw-Hill, N. Y., 1960, 4th ed., p. 201-203.

2. L. M. Milne-Thomson, Theoretical Hydrodynamics, The MacMillan Co., N. Y., 1964, 4th ed., p. 249-250.

3. A. E. Bryson, "Symmetric Vortex Separation on Circular Cylinders and Cones," Jour. Appl. Mechs., ASME, 643-648, (1959).

4. T. Sarpkaya, "Unsteady Flow Over Bluff Bodies," Developments in Mechanics, Pergamon Press, Oxford, England, 1964, p. 45-68.

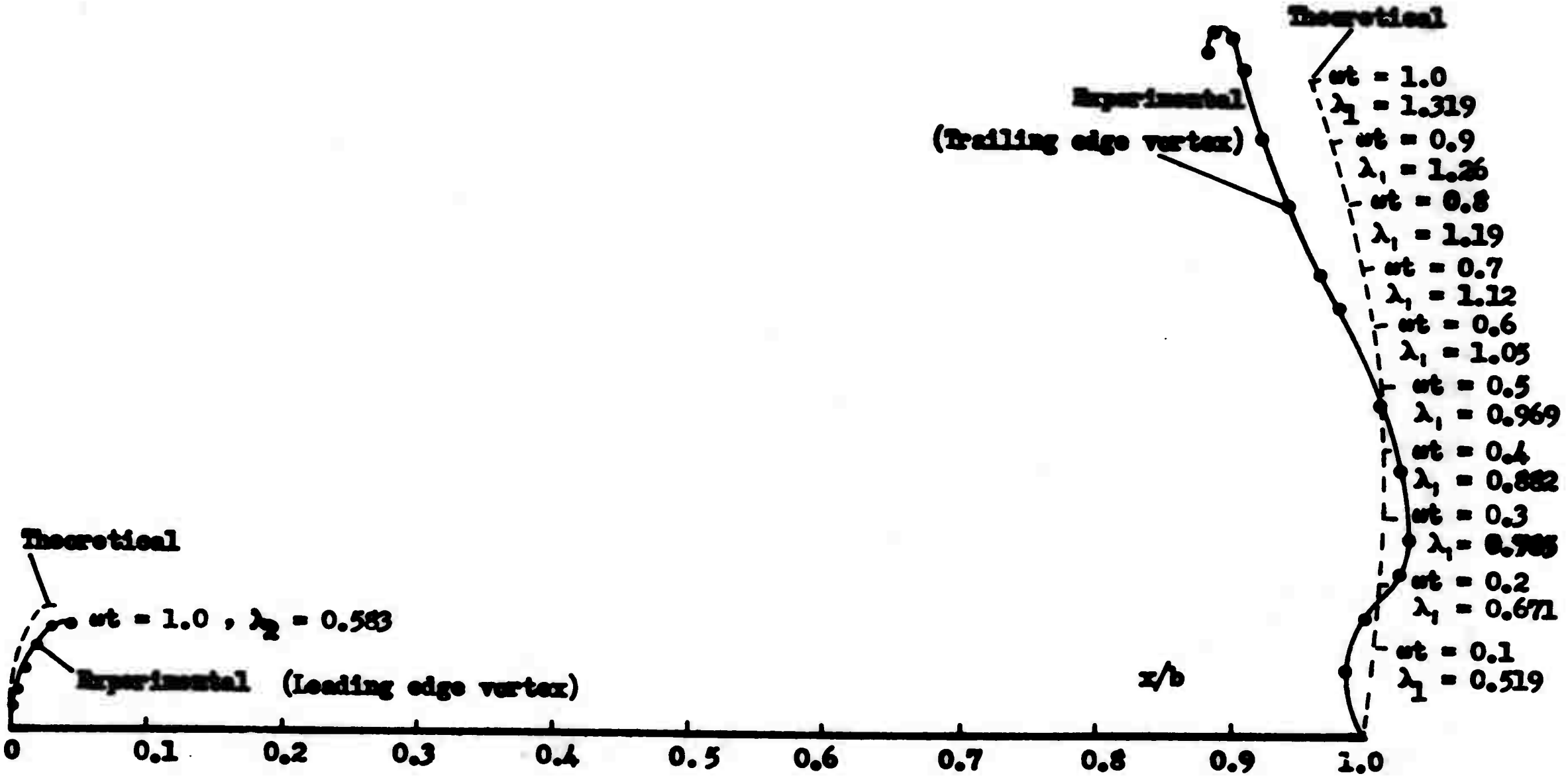

FIG. 2 LOCATION OF VORTICES

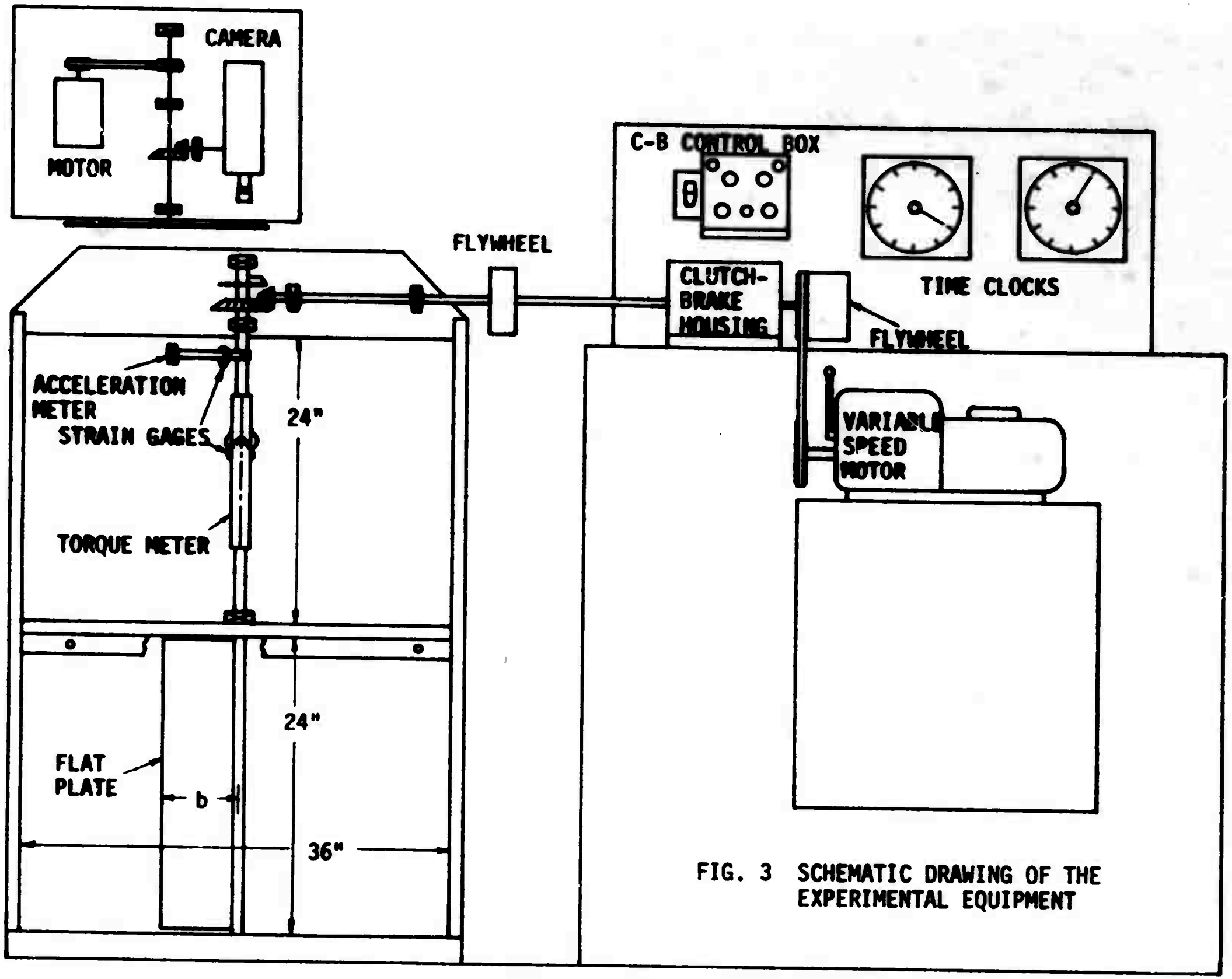

FIG. 3 SCHEMATIC DRAWING OF THE EXPERIMENTAL EQUIPMENT

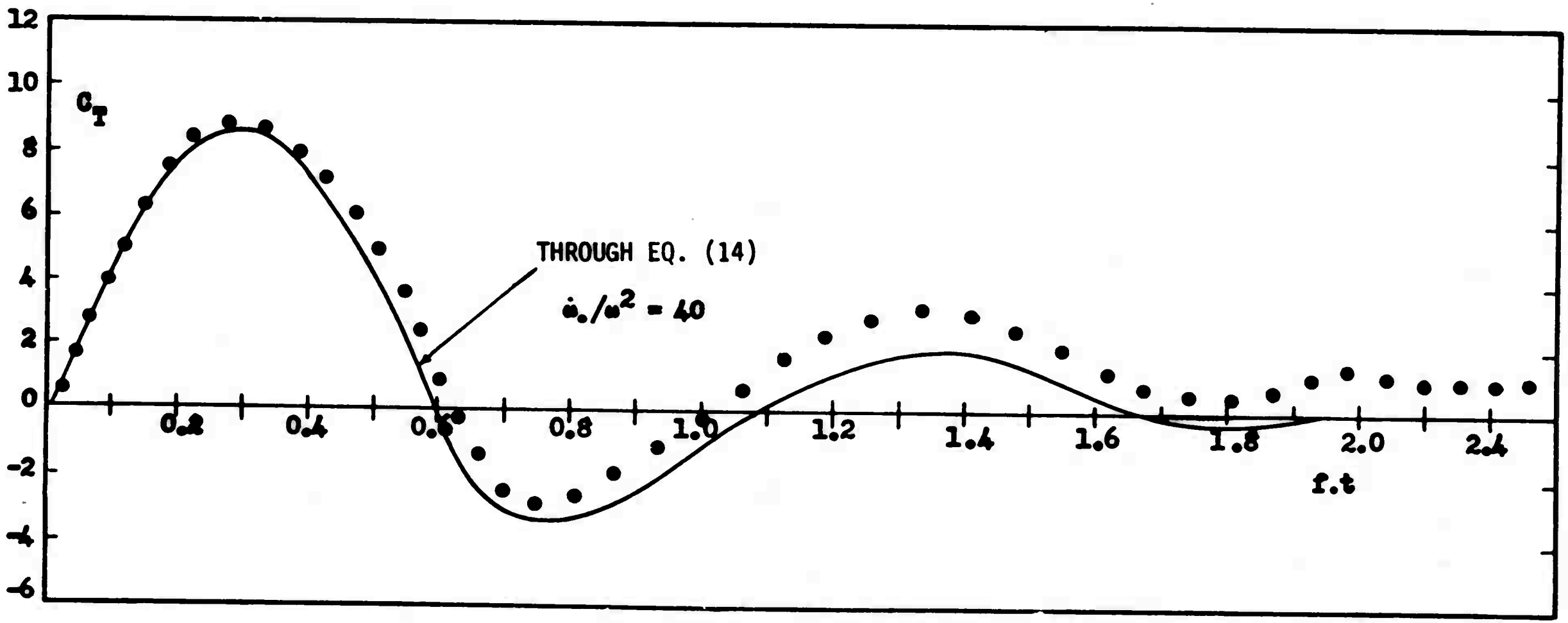

FIG. 4 TORQUE COEFFICIENT C_T AS A FUNCTION OF f.t

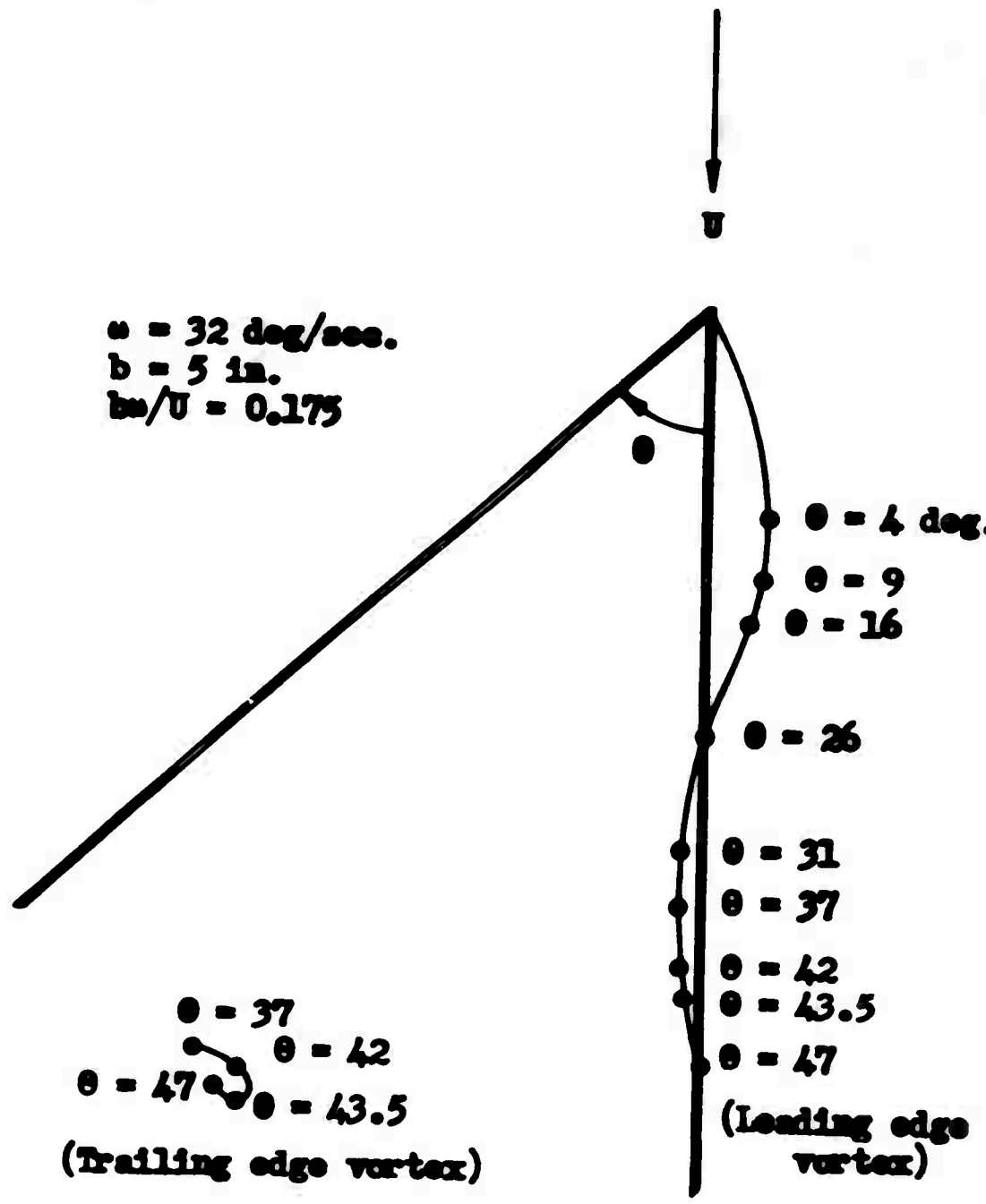

FIG. 5 LOCATION OF VORTICES

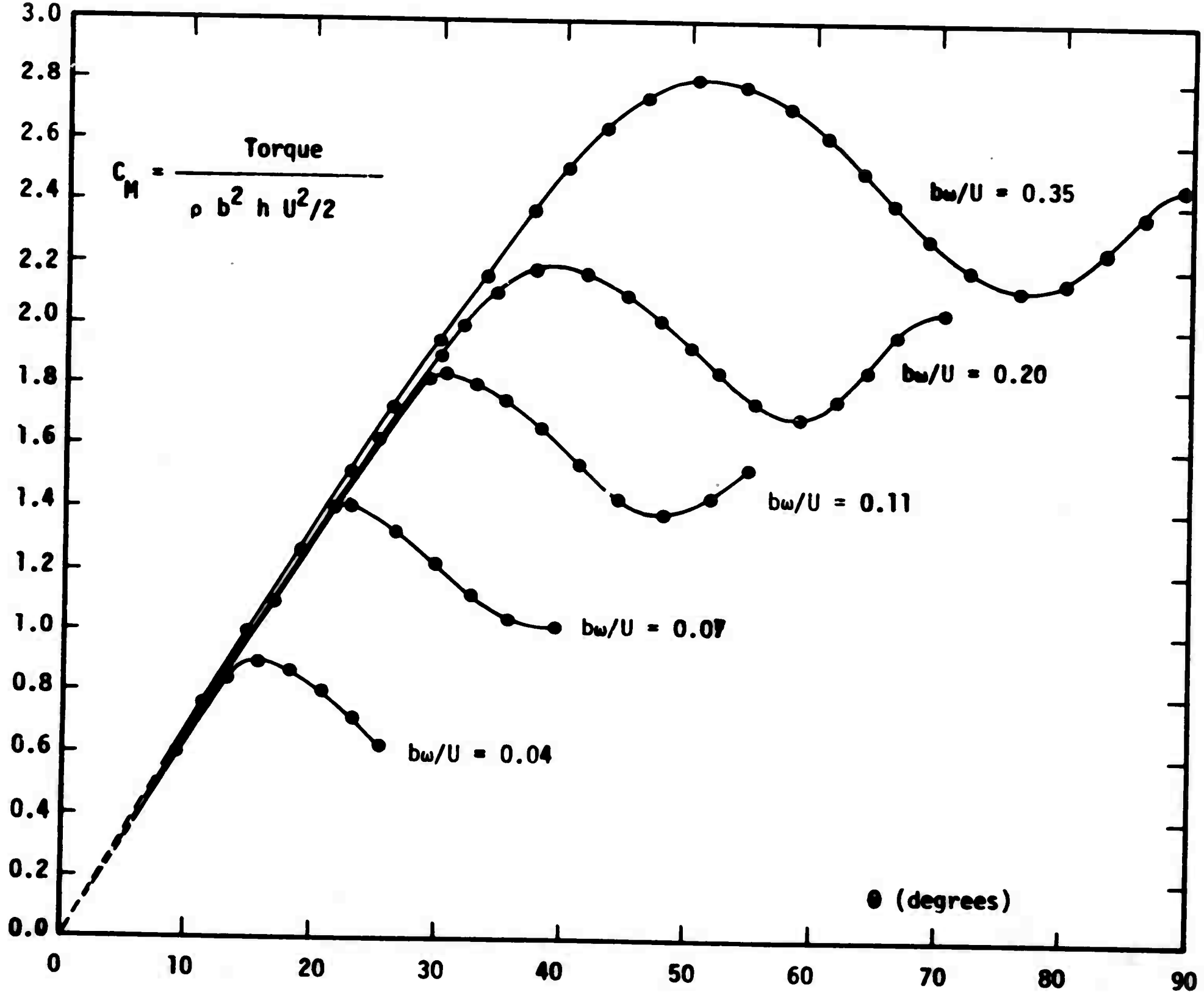

FIG. 6 TORQUE COEFFICIENT FOR A FLAT PLATE ROTATING IN STEADY UNIFORM FLOW